Extreme rainfall reduces one-twelfth of China's rice yield over the last two decades

Jin Fu, Yiwei Jian, Xuhui Wang, Laurent Li, Philippe Ciais, Jakob Zscheischler, Yin Wang, Yanhong Tang, Christoph Müller, Heidi Webber, et al.

Extreme rainfall reduces one-twelfth of China's rice yield

Jin Fu[1]†, Yiwei Jian[1]†, Xuhui Wang[1]†, Feng Zhou[1]*, Laurent Li[2], Philippe Ciais[3,4], Jakob Zscheischler[5], Yin Wang[6], Yanhong Tang[6], Christoph Müller[7], Heidi Webber[8], Bo Yang[9], Yali Wu[10], Qihui Wang[1], Xiaoqing Cui[1], Weichen Huang[1], Yongqiang Liu[11], Shilong Piao[1,12]

[1]Sino-France Institute of Earth Systems Science, Laboratory for Earth Surface Processes, College of Urban and Environmental Sciences, Peking University; Beijing, China.

[2]Laboratoire de Météorologie Dynamique, CNRS, Sorbonne Université; Paris, France.

[3]Laboratoire des Sciences du Climat et de l'Environnement, LSCE; Gif sur Yvette, France.

[4]Climate and Atmosphere Research Center (CARE-C), The Cyprus Institute; Nicosia, Cyprus.

[5]Department of Computational Hydrosystems, Helmholtz Centre for Environmental Research – UFZ; Leipzig, Germany.

[6]Institute of Ecology, Laboratory for Earth Surface Processes, College of Urban and Environmental Sciences, Peking University; Beijing, China.

[7]Potsdam Institute for Climate Impact Research (PIK), Member of the Leibniz Association, Potsdam, Germany.

[8]Leibniz Centre for Agricultural Landscape Research, Müncheberg, Germany.

[9]Key Laboratory of Nonpoint Source Pollution Control, Institute of Agricultural Resources and Regional Planning, Chinese Academy of Agricultural Sciences; Beijing, China.

[10]National Engineering Laboratory for Lake Pollution Control and Ecological Restoration, Chinese Research Academy of Environmental Sciences; Beijing, China.

[11]State Key Laboratory of Plant Genomics, Institute of Genetics and Developmental Biology, Chinese Academy of Sciences; Beijing, China.

[12]Key Laboratory of Alpine Ecology, Institute of Tibetan Plateau Research, Chinese Academy of Sciences; Beijing, China

†These authors contributed equally to this work.

*Corresponding author. Email: zhouf@pku.edu.cn

Extreme climate events constitute a major risk to global food production. Among these, the extreme rainfall is often dismissed from historical analyses and future projections, whose impacts and mechanisms remain poorly understood. Here, we find that rice yield reductions due to extreme rainfall in China were comparable to those induced by extreme heat over the last two decades, reaching 7.3 ± 0.7% (one standard error) according to nationwide observations and 8.1 ± 1.1% according to the crop model incorporating the mechanisms revealed from manipulative experiments. Extreme rainfall reduces rice yield mainly by limiting nitrogen availability for tillering that lowers per-area effective panicles and by exerting physical disturbance on pollination that declines per-panicle filled grains. Considering these mechanisms, we projected ~8% additional yield reduction due to extreme rainfall under warmer climate by the end of the century. These findings demonstrate the critical importance to account for extreme rainfall in food security assessments, posing greater challenges to climate change adaptation.

Extreme climate events have been recognized as a major risk induced by climate change[1]. Agricultural ecosystems are among the most vulnerable to climate extremes, resulting in remarkable damage to crop production[2,3]. For example, extreme climate events have been shown to account for 18-43% of the observed anomalies in global crop yields[4]. The consequences of such yield anomalies vary from fluctuations in food prices, destabilized food supply, to famines[5]. As such, understanding the impacts of extreme climate events on crop yield is critical for adapting food systems to future climate change and thus contributing to food security for the growing global populations. Recent studies have focused on elucidating impacts of drought[6,7], extreme heat[8,9] and cold spells[10], but the impact of extreme rainfall on yields remain largely uncertain[11,12].

Estimating the yield loss due to extreme rainfall needs to assess the magnitude of extreme rainfall and timing of crop exposure, both of which are highly heterogeneous over space and time. Spatially, previous studies based on yield statistics and climate variables aggregated at administration zones may have smoothed out the highly localized extreme rainfall events, resulting in minimal impact of extreme rainfall being detected (−0.6 ± 1.2%, mean ± standard error), which is far below the observational damages from other climate extremes (e.g., −8.1 ± 3.1% from extreme heat, −5.2 ± 2.8% from drought, and −10.2 ± 6.5% from extreme cold; Supplementary Table 1). Temporarily, the exposure of crops to extreme rainfall can be dismissed if using climate data with coarse temporal resolution to explore the climate-yield relationships[3]. The

lack of clear mechanistic evidence for extreme rainfall impacts[4,11] has also rendered crop modelers to dismiss their potential effects in projecting the impacts of climate change[13], despite the expected increase in occurrence of extreme rainfall[14].

Rice is the primary calorie source for more than 50% of the world's population, with the largest production in China[15]. Rice is generally considered to be strongly tolerant to extreme rainfall, though this may be an artifact of relatively intense irrigation and drainage management that minimizes adverse effects of rainfall anomalies[16,17]. As a result, extreme rainfall impacts on rice yield remain poorly investigated. Here, we used long-term nationwide observations and multi-level rainfall manipulative experiments to explore the magnitude and mechanisms of extreme rainfall impacts on rice yield in China (see Methods, Supplementary Figs 1 and 2). We further improved a process-based crop model by explicitly accounting for the relevant mechanisms to hindcast and project the yield responses to extreme rainfall across China. This combination of field observation, manipulative experiment, and model simulation enables us to address three questions here: what is the magnitude and pattern of change in rice yield due to extreme rainfall? what are the key mechanisms determining rice yield response to extreme rainfall? how strongly do changes in extreme rainfall impact future rice yield?

Evidence from nationwide observations

We used a window searching strategy[18] to isolate change in rice yield (ΔY) induced by

each extreme climate event for specific site and year combinations from the nationwide observations (see Methods, an example in Supplementary Fig. 3, and the definition of events in Supplementary Table 2). ΔY is defined as the relative change in rice yield between the treatment and control cases (in %), after excluding the effects from the other meteorological indicators and changes in rice cultivar and phenology, where in the treatment rice has been exposed to a given extreme event during the rice growing season, and in the control rice has not been exposed to that event and other extreme events either did not occur or were the same as in the treatment. This yielded 707 ΔY data at 114 sites covering most of rice production areas in China (Supplementary Fig. 1b). These data show that extreme rainfall induced a significant yield reduction by 7.3±0.7% (one standard error) in China (n = 217, P < 0.001, Fig. 1a). Such yield reduction is roughly equivalent to 9 times the annual rice yield growth over the past three decades (0.8% yr^{-1}, Supplementary Fig. 4). Counter-intuitively, the yield reduction due to extreme rainfall was comparable to that due to extreme heat (5.0±1.8%, n = 61), and larger than the reductions related to drought (4.4±1.0%, n = 152), extreme cold (3.7±0.8%, n = 163), and the other extreme events (e.g. hail, typhoon and tropical cyclones, 2.5±1.2%, n = 114, Fig. 1a). The larger ΔY for extreme rainfall in relative to other extreme events is robust when comparing different extreme events with similar probability of occurrence (Supplementary Fig. 5). Spatial analyses further confirm that the negative effects of extreme rainfall on rice yield are more pervasive and stronger than those of other extreme events, even though record yield reductions (ΔY < –20%) can arise from any type of extreme events considered here (Fig. 1b-f).

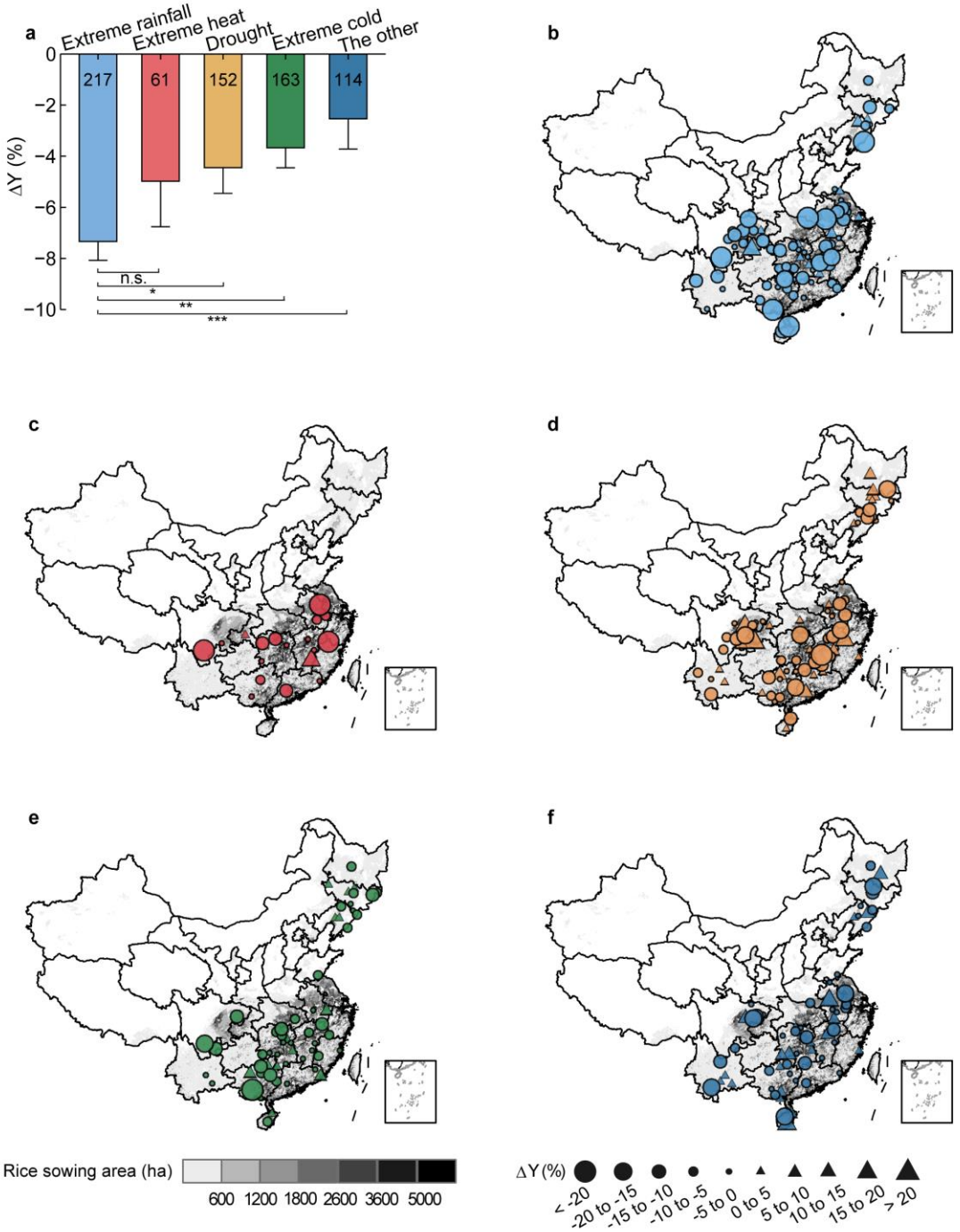

Fig. 1. Changes in rice yield (ΔY) induced by extreme climate events in China. **a**. The mean and standard error of ΔY from 1,000-time bootstrap estimates. **b-f**. Pattern of ΔY induced by extreme rainfall, extreme heat, drought, extreme cold, and the other events (typhoon and tropical cyclones), respectively. The digits noted at the base of each bar in panel **a** are the number of ΔY. The Asterisks refer to statistical significance of the differences in mean ΔY between extreme rainfall and other events based on the Wilcoxon rank sum test, with * $P < 0.05$, ** $P < 0.01$, *** $P < 0.001$, and n.s. for not significant. ΔY in panels **b** to **f** is presented for each site, but averaged in case of multiple samples.

To identify the potential factors determining the magnitude of extreme rainfall impacts, correlation analyses were performed between ΔY and extreme rainfall parameters. We define extreme rainfall as the 99th percentile of hourly precipitation during rice growing season for each site (see Methods). The analyses show that extreme rainfall induced ΔY was negatively correlated with the intensity (cm per hour), the event amount (cm per event for which the break between hourly precipitation lies below 6 hours), and the event duration (hour per event) of extreme rainfall, rather than with the total intensity, frequency or proportion of extreme rainfall (Supplementary Fig. 6). The combining results from the Kruskal-Wallis Rank Sum Test and the Dunn's test affirmed that the repeated extreme rainfall does not add to additional yield loss (Supplementary Fig. 6g). These relationships are robust against variations in the definitions of extreme rainfall (95th, 99th or 99.9th percentile) and of break duration (2, 6 or 12 hours) for consecutive extreme rainfall events (Supplementary Table 3), confirming the key driving indicators are hourly intensity and event amount rather than repeated frequencies. The sensitivities of ΔY to extreme rainfall intensity and event amount were −1.6 ± 0.7 % (cm h^{-1})$^{-1}$ and −0.4 ± 0.1 % cm^{-1}, respectively (Supplementary Fig. 6a, d). Such a sensitivity of ΔY to rainfall intensity is roughly in line with previous field observations (−1.0 ± 0.2 % (cm h^{-1})$^{-1}$, n = 11), but larger than the results from previous statistical analysis aggregated at administrative scales (−0.03 ± 0.05 % (cm h^{-1})$^{-1}$, n = 33; Supplementary Table 1).

Experimental tests of the extreme rainfall-rice yield relationship

To isolate the mechanisms leading to extreme rainfall impacts on ΔY, we established a

series of rainfall manipulative experiments in 2018 and 2019 (see Methods and Fig. 2a for detailed setup). In the experiments, we established four rainfall levels to broadly represent extreme rainfall events across China's rice fields. To test if the impacts differ by growth phases, rainfall manipulation was conducted for each or their combination of the three phases (i.e., vegetative phase when tillers are formed, reproductive phase when spikelets reach anthesis, and ripening phase when grains are filled). We quantified ΔY between treatment and control plots for which two replicates were considered. In agreement with the nationwide observations, ΔY was −1.1 ± 0.3% and −0.6 ± 0.1% in response to 1-centimeter increase in extreme rainfall intensity and event amount, respectively. These effect sizes were also statistically the same between the two experimental years (Supplementary Fig. 7a, b). Analyses of changes in yield components indicated that ΔY were mostly caused by declines in effective panicles per unit land area (EP) and filled grains per panicle (FG), accounting for 22% to 25% and 71% to 75% of ΔY, respectively, whereas decreased grain weight (GW) only contributed to approximately 1.4% to 6.0% (Fig. 2 and Supplementary Fig. 7c). Extreme rainfall impacts on yield components depend on growth phase. Extreme rainfall in the vegetative phase mainly reduced EP, while in the reproductive phase, it mainly reduced FG. (Fig. 2).

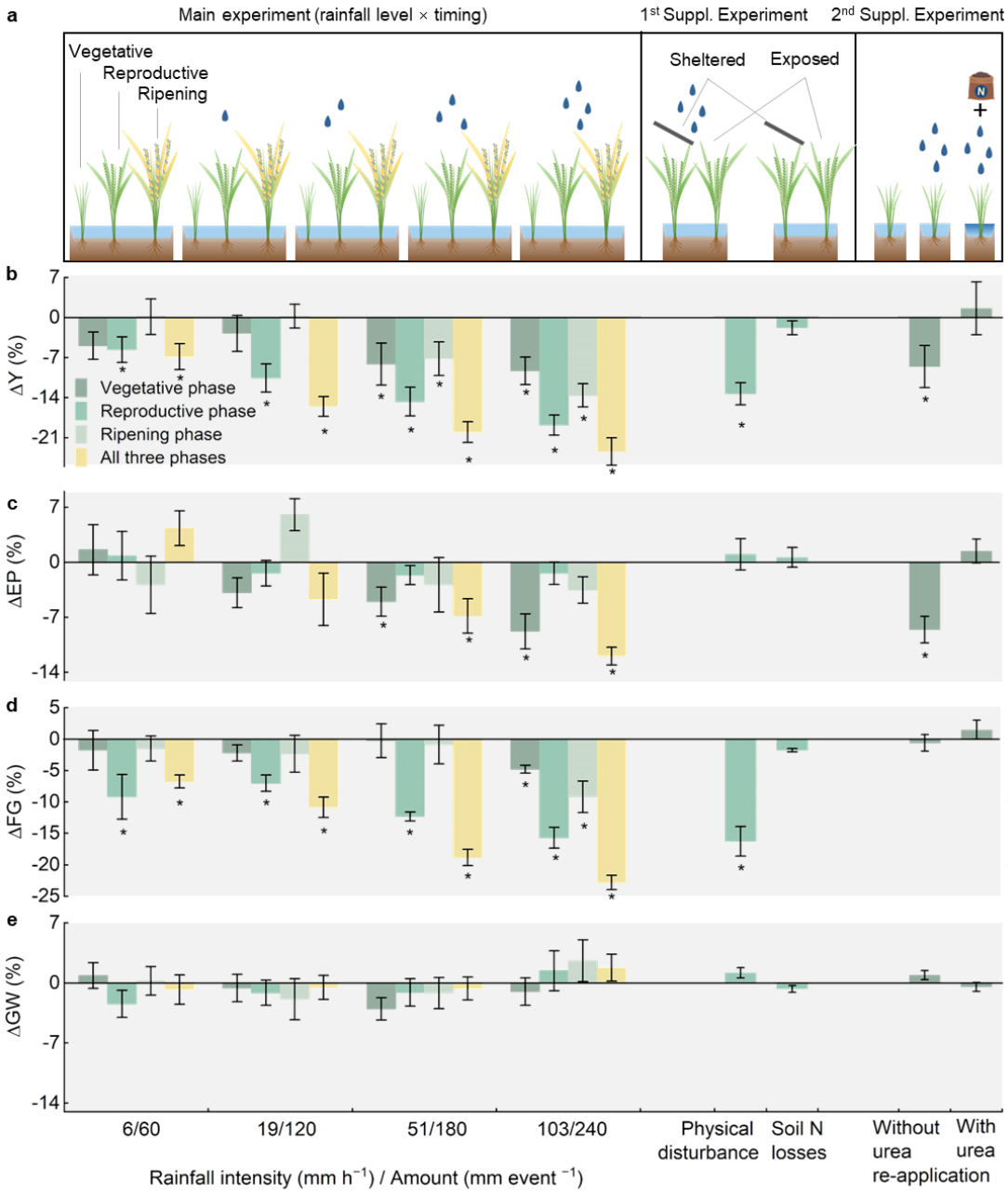

Fig. 2. Effects of simulated rainfall on rice yield and yield components. **a**. Experimental setup. **b** to **e**. Relative changes in rice yield (ΔY), effective panicles per unit land area (ΔEP), filled grains per panicle (ΔFG), and grain weight (ΔGW), respectively. For the 2nd supplementary experiment, the urea re-application rate (i.e., 28.8 kg N ha^{-1}) is equal to the average N losses observed from the treatment plots using the same rainfall amount during vegetative phase in main experiments. Asterisk indicates for the significant difference with zero, with $P < 0.05$.

We hypothesized that the growth phase-dependent effects of extreme rainfall result from different mechanisms in reducing rice yield, that is, high extreme rainfall intensity

142 reduces FG through physical disturbance (in terms of kinetic energy) on pollination[19,20],
143 and high extreme rainfall event amount stresses tillering through inducing soil N
144 losses[21,22]. To test these hypotheses, we conducted two supplementary experiments
145 using the maximum rainfall level (103 mm per hour for intensity or 240 mm per event
146 for event amount) in 2021 (see Methods).

147

148 In the first supplementary experiment, we sheltered half of each rice plot during the
149 reproductive phase so that the sheltered halves of treatment were affected by extreme
150 rainfall only through its effects on soil N losses, but not direct physical disturbance (Fig.
151 2a and Supplementary Fig. 8). We found FG in the sheltered halves of treatment show
152 little difference (< 2.0%) with the control, while FG in the exposed halves of treatment
153 decreased by 18.0 ± 2.6% (Fig. 2). The empty or shrunken grains were found mostly in
154 the upper part of the panicles of the exposed halves of treatment (Supplementary Fig.
155 9), further supporting that FG were reduced by the physical disturbance that prevents
156 successful pollination, a critical process of yield formation.

157

158 The second supplementary experiment isolates the effects of soil N losses induced by
159 extreme rainfall event amount during the vegetative phase (Supplementary Fig. 8a). We
160 supplied additional urea to half of the treatments, so that if there was a soil N loss
161 induced by the extreme rainfall, it would be compensated. We found that urea re-
162 application could help maintain N uptake per tiller, and thus successfully stabilized EP

and rice yield (Fig. 2). Treatments that did not compensate for N losses caused proportionally similar declines in N uptake per tiller and thereby EP (R^2 = 0.70 and 0.57, respectively, $P < 0.001$, Supplementary Fig. 10). These findings confirm that the reduced EP was primarily attributable to extreme rainfall event amount that limits soil N availability and crop N uptake causing lower yields.

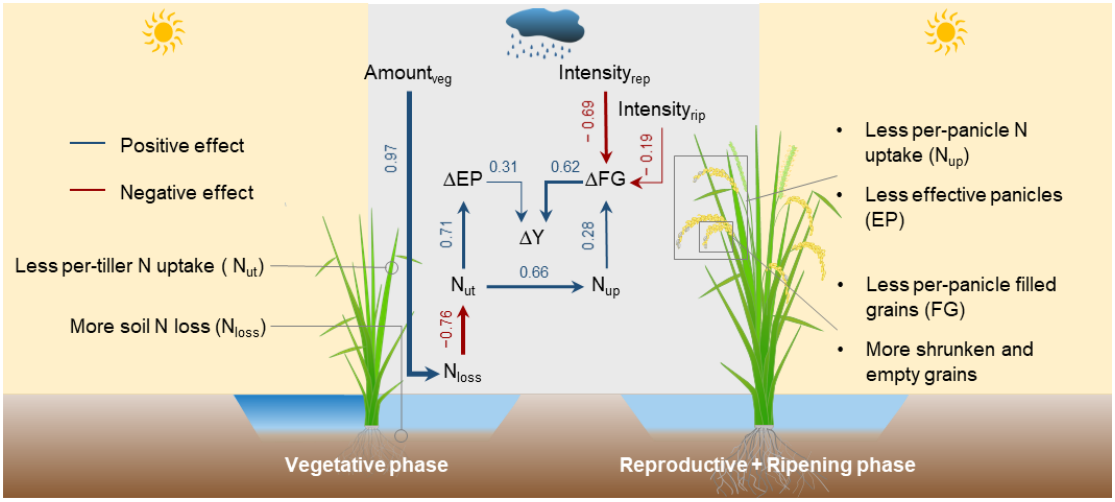

Fig. 3. Schematic diagram of extreme rainfall impacts on rice yield. Single-headed arrows indicate the direction of causation identified by the structural equation modelling. Blue (red) arrows indicate significant positive (negative) effects ($P < 0.05$). Arrow width is proportional to the strength of the relationship, which is characterized by standardized path coefficients showing next to arrows. Amount$_{veg}$, extreme rainfall event amount in vegetative phase; Intensity$_{rep}$ and Intensity$_{rip}$, extreme rainfall intensity in reproductive and ripening phases, respectively; ΔY, relative changes in rice yield.

Ultimately, we summarized and tested our findings from the experiments with structural equation modelling (SEM) to illustrate the mechanisms by which extreme rainfall reduces rice yield (Fig. 3). The SEM including the direct pathways of rainfall-induced physical disturbance and soil N losses shows the best performance (Supplementary Fig. 11a), explaining 56% of the overall variance in rice yield reductions. This suggests that both pathways are primary mechanisms explaining ΔY, whereas other potential

mechanisms (e.g., changes in photosynthesis, leaf area index, phosphorous loss, phosphorous and potassium absorptions) do not show significant effects (Supplementary Fig. 11b-f). In addition to these two pathways, the best-fit SEM also identified an indirect pathway, i.e., rainfall-induced N losses during the vegetative phase, which may also limit per-panicle N uptake during the reproductive phase thereby decreasing FG (Fig. 3 and Supplementary Fig. 11a).

Crop model improvements for assessing ΔY

Correctly representing the mechanisms through which extreme rainfall reduces rice yield is critical for diagnosing and projecting spatiotemporal variations in rice yield. We introduced the first physical disturbance module of extreme rainfall on rice yield in ORganizing Carbon and Hydrology in Dynamic EcosystEms for crops (ORCHIDEE-crop)[23], which is a process-based crop model including the representation of single, early and late rice types, paddy rice irrigation, and a detailed soil hydrology model[24]. The direct and indirect pathways of extreme rainfall through soil N losses was also introduced into the model (see Methods and Supplementary Table 4). The improved model can robustly capture the observed rice yield variability due to year-to-year climate variations and extreme rainfall treatments (the coefficient of determination of 0.88 in 2018 and 0.78 in 2019, mean root square error of 0.69 in 2018 and 1.19 in 2019, Supplementary Fig. 12). The model was further validated by field observations of rice yield in 2021 between control and treatment (Supplementary Fig. 12).

We then used the high-resolution global precipitation measurement (GPM) datasets[25] to drive the improved model over China in 2001-2016 (see Methods). On average, the improved model hindcasts lower rice yields due to the extreme rainfall by 8.1 ± 1.1% (one standard error for interannual variability) for all rice types, 8.3 ± 1.0% for single rice, 8.6 ± 1.0% for early rice, and 7.6 ± 1.3% for late rice (Supplementary Fig. 13a-c). Higher ΔY were simulated eastern China and southern coastal regions which experienced higher rainfall intensities (Supplementary Fig. 13a-c). Factorial model simulations show that physical disturbance induced by extreme rainfall was the most important determinant across 47-95% of rice sowing areas (Supplementary Fig. 13d-f), leading to yield losses of 3.9% for single rice, 5.1% for early rice, and 4.1% for late rice. Extreme rainfall-induced N losses dominated the ΔY mainly in Anhui and Jiangsu provinces where both N application rates[26] and extreme rainfall event amount were relatively high[27] (Supplementary Fig. 13h-j).

Projected impacts of future change in extreme rainfall

Since extreme rainfall was found to have significant impacts on historical rice yields, a process which was neglected in previous projections under climate change[28,29], we made a first attempt to project the risk of future rice yield to changing extreme rainfall dynamics. We used the high-resolution climate projection by the IPSL model zoomed over China[30], which performed well in reproducing the spectral properties of rainfall

including extreme events[31], to drive the improved model under two climate scenarios (representative concentration pathways [RCP] 4.5 and 8.5; see Methods). Considering extreme rainfall impacts led to greater projected yield reductions by the end of this century (2085-2100, Fig. 4). On average, extreme rainfall induces an additional yield reduction of 7.6% in China on the top of other climate-change induced impacts under RCP 4.5. We then ranked the additional yield reductions in grid cells from the largest to smallest and calculated the cumulative sowing area affected by a given additional yield change, and found that the sowing areas with additional yield reduction of >7.6% accounted for 58% for early rice, 39% for single rice, and 29% for late rice (Fig. 4a). Rice is projected to suffer from extreme rainfall events the most over northeast China and southeast coastal regions (Fig. 4b-d). However, additional yield reductions were projected to be weaker under RCP 8.5 relative to RCP 4.5 (Fig. 4e-h), with the national mean reduction due to extreme rainfall of 5.4%, mainly because of larger rice yield reduction induced by stronger warming and carbon dioxide concentrations under RCP 8.5 together with no differences in projected extreme rainfall between the two scenarios (Supplementary Fig. 14). These new projections highlight the increasing risk of rice yield reductions induced by extreme rainfall and an urgent need to consider this risk in planning climate change adaptations.

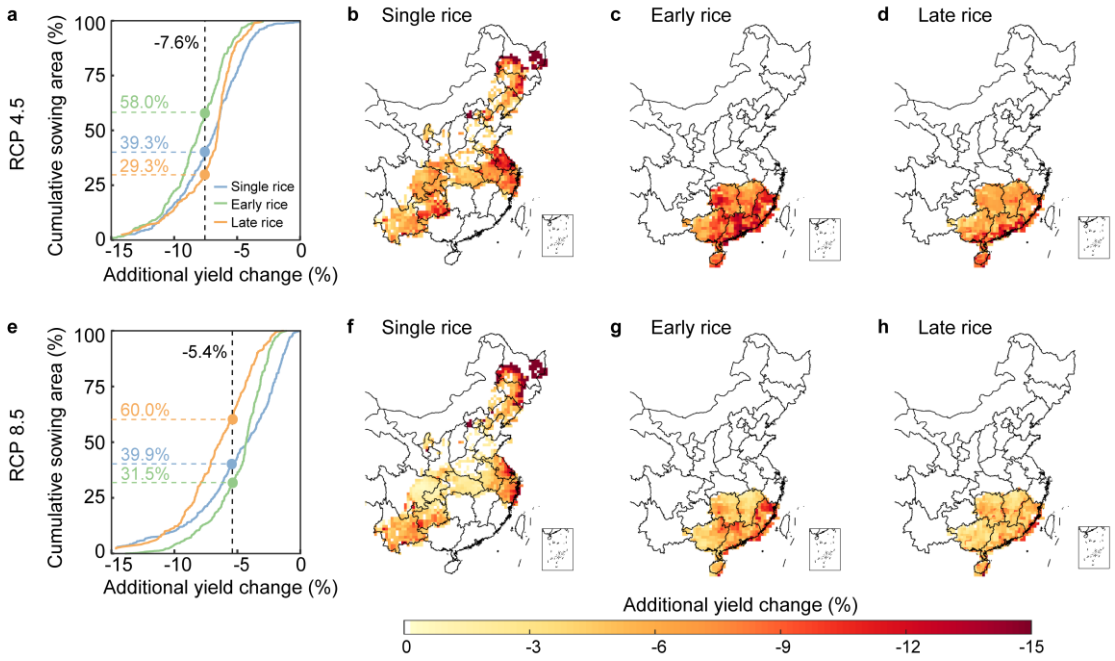

Fig. 4. Future projections of additional yield change induced by extreme rainfall. **a** and **e.** cumulative proportions of sowing area affected by a given additional yield change under RCP 4.5 and RCP 8.5, respectively; Black dashed lines represent the national means (–7.6% and –5.4%), and the numbers represent the cumulative proportions of sowing area affected by exceeding the national means. **b** to **d**. Patterns of ΔY under RCP 4.5. **f** to **h**. Same as panels **b** to **d** but under RCP 8.5.

Discussion

While both nationwide observations and model simulations indicated approximately 8% of rice yield lost in China due to extreme rainfall, we note that our analyses are subject to several sources of uncertainties. On the observation side, due to rigorous screening criteria to isolate extreme rainfall impacts from other extreme events, rice yield assessment has been eliminated over the Southeast Coast where extreme rainfall is strong (Supplementary Figs 1b and 15), likely underestimating the extent of extreme rainfall induced ΔY. On the modelling side, extreme rainfall intensity and event amount used for driving the historical simulations across China were from the half-hourly and 0.1-degree GPM dataset, which is well represented for but still did not fully capture the

observed heaviest rainfall extremes (Supplementary Fig. 16). Thus, our estimates of extreme rainfall impact on rice yield should be viewed as a conservative assessment. Another source of uncertainty is related to the setup of our manipulative experiments. The experiments were conducted on cloudy days to approximate natural rainfall conditions, but muted the effects of accompanying processes such as reduced air temperature[32] and enhanced waterlogging[33]. These accompanying processes may cause rice diseases and lodging that can further compound rice yield responses[12,34]. Moreover, our experiment focused on uncovering mechanisms of extreme rainfall impacts under regular management, without climatic adaptations, which introduces additional uncertainties in future projection.

Although we focused on rice yields in China that is the largest rice producer globally, attention to other rice producing regions may yield critical insights into the biogeography and generalizability of our findings. Compared to China, rice fields in South and Southeast Asia have smaller N application rates and larger fractions of rainfed rice (Supplementary Fig. 17). Extreme rainfall in these regions may lead to a lower risk of soil N losses and thus lower impacts on tillering. However, these regions were more exposed to extreme rainfall given much higher extreme rainfall intensity (Supplementary Fig. 15b), and thus subject to higher risk of physical disturbance. Since across approximately 80% of China's rice fields, extreme rainfall impacts results from direct physical disturbance on pollination, rice yield reductions in South and Southeast Asia should also be significant. Previous projection of rice yield response to climate

284 change without considering the extreme rainfall impacts (e.g., Webber et al.[13],
285 Rosenzweig et al.[28], Jägermeyr et al.[29], Iizumi et al.[35]) have likely been overly
286 optimistic in this regard.

287

288 The impacts of extreme rainfall on other staple crops such as wheat and maize remain
289 to be explored. Although the magnitude and mechanistic representation of rice yield
290 response to extreme rainfall may not be directly applicable to other crops, our research
291 paradigm that combines field observations, manipulative experiments, and processed-
292 based modelling is well transferable. Unlike rice, sizable fraction of upland crops were
293 rainfed or under different irrigation-drainage systems[36]. The sensitivity of tillering and
294 pollination processes in response to extreme rainfall may also be different from what
295 we observed here. Therefore, a major research challenge remains to assess the global
296 extreme rainfall impacts for all cereal crops.

297

298 # Methods

299 **Analysis of nationwide observational data**

300 *Yield change induced by extreme climate events*. We collected field observations of rice
301 yield and extreme climate events from the national agrometeorological observation
302 network that is run by the China Meteorological Administration (CMA). This network
303 covers most rice production areas, including single rice in northeast and central China
304 and early and late rice in south China (Supplementary Fig. 1a). It provides rice yield of

2,304 site-year records from 166 sites, and extreme climate events of 8,595 records from 356 sites occurred in the rice growing seasons over the period 1999-2012. Rice yield is defined as actual production divided by the hectare of harvested area. Extreme climate events are recorded on given days for each site and are sorted into five broad categories, i.e., extreme heat, extreme cold, extreme rainfall, drought, and the other events (see definitions in Supplementary Table 2).

First, the field observations are reproduced by summing the detrended yield and the multi-year average (Y_{de}) for each site and rice type, to avoid the impacts of changing rice cultivar, phenology and technology. Second, to exclude the effects of the other meteorological indicators on yield, a multiple linear regression analysis is applied for Y_{de} against mean temperature, total precipitation and total sunshine hours during rice growing season for each site and rice type. Regression coefficients are determined as the median of 1,000-time bootstrap estimates, and used for predicting yield ($Yfit_{de}$). Third, a window searching strategy[18] is applied to find all available control-treatment pairs (*YC* and *YT*) to quantify rice yield change (ΔY) induced separately by different extreme events for a given site and year (Supplementary Fig. 3):

$$\Delta Y = \frac{(YT_{de} - YTfit_{de}) - (YC_{de} - YCfit_{de})}{YC_{de}} \times 100\% \quad (1)$$

This strategy expands on previous studies[3,11,12,37-42] in at least three aspects: (i) It ensures both control and treatment sharing approximately the same management practices (e.g., fertilization, irrigation, and drainage) and geographical conditions (e.g., soil properties and topography), while almost avoiding technology- or cultivar-driven

change in rice yield; (ii) it isolates the impact of a given extreme event on rice yield while largely reducing the noise due to the other events, and (iii) it provides an observational evidence for climate extreme impacts on rice yield at the site scale, rather than expected signal from statistical inferences at administrative scales. Finally, a dataset of 707 control-treatment pairs from 114 sites were identified, i.e., 217 pairs for extreme rainfall at 82 sites, 152 pairs for drought at 73 sites, 61 pairs for extreme heat at 18 sites, 163 pairs for extreme cold at 61 sites, and 114 pairs for the other events at 68 sites (Supplementary Fig. 1b and Data 1).

The Wilcoxon rank sum test was applied to assess the significance of ΔY. The choice is motivated by the fact that ΔY is not normally distributed (Kolmogorov-Smirnov test, $P < 0.05$). The Wilcoxon rank sum test was also applied to quantify the difference between extreme rainfall and other extreme events. To solve the inconsistency of sample size among the extreme events, we applied the bootstrap resampling to estimate the means and standard error of ΔY by randomly sampling an equal size from the initial dataset for 1000 times. The results show that the differences in ΔY are robust, because ΔY are dominated primarily by climate extremes with moderate effects on rice yields, rather than a few outliers (Supplementary Fig. 18), and are not strongly influenced by sample size (Supplementary Fig. 19). In addition, we calculated the percentiles of the extreme events occurred in the period 1999-2012, and found that most of them exceed 95th percentile (Supplementary Fig. 5a-d). However, these percentiles are not completely consistent among the events. To test the robustness of the differences in ΔY, we

compared the effects of different extreme events with similar percentiles, that is, 95th to 99th (or 99th to 99.8th) percentiles for extreme heat and rainfall and 1st to 5th (or 0.2nd to 1st) percentiles for extreme cold and drought (Supplementary Fig. 5e-f).

Sensitivity of ΔY to extreme rainfall. We defined extreme rainfall if hourly precipitation exceeds the threshold that is the 99th percentile of growing-season hourly precipitation over the reference period 1981–2012 for each site. The data for hourly precipitation were acquired from the CMA. To outstand the main influencing factors, seven extreme rainfall parameters, reflecting characteristics of intensity, event amount and repeated extreme rainfalls, were then quantified during rice growing season for each treatment (Supplementary Data 1), including intensity as the maximum hourly precipitation when exceeding the threshold (RX1h, cm h^{-1}), total intensity as the sum of hourly precipitation when exceeding the threshold (RX1hTOT, cm h^{-1}), frequency as hours or the fraction of the hours when hourly precipitation exceeds the threshold to the length of rice growing season in hours (R99f, hours, and R99p, %) , proportion as the sum of hourly precipitation that exceeds the threshold divided by the growing-season total precipitation (R99pPROP, %), event amount as the precipitation amount averaged for extreme rainfall events that involve at least one extreme rainfall and for which the break duration between hourly precipitation does not exceed 6 hours[43] (Rg1event, cm per event), and event duration as the total hours of extreme rainfall events during rice growing season divided by event numbers (ERED, hour per event).

We then conducted correlation analyses of the extreme rainfall induced ΔY against seven parameters for identifying the potential factors. The correlation emphasizes the changes in rice yields caused by the maximum precipitation intensity and event amount, rather than repeated extreme rainfall events nor proportion to total precipitation amount, though it may be also affected by large values of parameters over a few sites. To tackle this uncertainty, we applied the bootstrap resampling to estimate the sensitivities and standard error of ΔY in response to extreme rainfall by randomly sampling 90% of the samples from the initial dataset for 1000 times. Besides, Kruskal-Wallis Rank Sum Test and Dunn's test are applied to confirm the insignificance of extreme rainfall frequencies (1, 2, 3 and ≥4 times) on ΔY. We also tested if ΔY response to extreme rainfall is dependent on the definitions of extreme rainfall. The sensitivity analyses were conducted based on the different thresholds (95^{th}, 99^{th} or 99.9^{th} percentile) to define extreme rainfall and based on the break duration (≤ 2, 6, or 12 hours) to define extreme rainfall event (Supplementary Table 3).

Rainfall manipulative experiments

Plants and cultivation condition. The experimental site is at the Jingzhou Agrometeorological Experimental Station in Hubei province, China (30°21′N, 112°09′E; Supplementary Fig. 2a). It is characterized as subtropical humid monsoon climate, with a mean air temperature of 16 °C and a mean precipitation of 1,095 mm yr^{-1}. Soil is classified as Hydragric Anthrosol (Supplementary Table 5). Rice seedling nurseries were managed under the water regime of continuous flooding. Seedlings of

393 rice (*Oryza sativa* L.) were transplanted at 30-day seedling ages with a hill spacing of
394 0.33 × 0.33 m (9 hills m^{-2}), and harvested after 103 days. Fertilizers of 172 kg ha^{-1} N
395 in the form of N-NH_4, 61 kg ha^{-1} P in the form of P_2O_5 and 49 kg ha^{-1} K in the form of
396 K_2O were applied over three events, that was one event with 72 kg ha^{-1} N, 53 kg ha^{-1} P
397 and 42 kg ha^{-1} K applied 1 day before rice transplanting, one with 78.7 kg ha^{-1} N
398 applied two weeks after transplantation, and one with 20.9 kg ha^{-1} N, 8 kg ha^{-1} P and
399 7 kg ha^{-1} K applied during the jointing stage. Further details on cultivation condition
400 can be found in Supplementary Fig. 2b.
401
402 *Main experiment*. The rainfall manipulative experiment was conducted from 2018 to
403 2019, spanning two rice growing seasons. The experiment consisted of ambient control
404 and factorial treatments with two replicates, and was designed for extreme rainfall
405 level-timing combinations (Supplementary Fig. 2c), with the results in Supplementary
406 Data 1. The treatments comprised four rainfall levels in each or all of three growth
407 phases (i.e., vegetative, reproductive, or ripening phases). There was a total of 34 plots
408 for main experiments, each of which had an area of 6 m^2 (2 m × 3 m) and was
409 completely isolated by plastic-covering levees and impervious plates at a 0.5-meter
410 distance in between. Throughout the experiment, all plots were subjected to the same
411 agricultural management practices. To avoid the border effects, we use independent-
412 samples t-test to compare the yield of ambient control with that of three plots nearby,
413 with each plot owing 150 m^2 (25 m × 6 m) with the same agricultural management
414 practices, and found no significant differences during three rice growing seasons

(P >0.05, Supplementary Fig. 20a).

We manipulated rainfall levels by running the artificial rainfall manipulation system (NLJY-10, Nanlin Electronics, China) for one hour on two replicates for each treatment, with the rainfall amount of 60, 120, 180, and 240 mm. However, the intensities of manipulative rainfall were far less than natural one because of a lower falling velocity of raindrops. We thus measured the kinetic energy of manipulative rainfalls using the laser precipitation disdrometer (OTT Parsivel^2, Hach, USA), which is equivalent to the natural rainfall intensities of 6, 19, 51, and 103 mm per hour. These rainfall levels represent most of the broad range of growing-season rainfall extremes (exceeding the 99th percentile) across China's rice fields (i.e., 8 to 143 mm per hour and 12 to 526 mm per event observed in the period 1999-2012). To approximate the natural rainfall condition, rainfall manipulation was conducted in cloudy daytime for vegetative and ripening phases, but for reproductive phase specifically at 8:00-13:00 when spikelets reach anthesis in experimental site. To minimize the impact of waterlogging, ponded water was discharged within 12 hours after rainfall manipulation if the depth exceeds 100 mm. No plants were washed away or fell due to rainfall manipulation.

For each plot, we measured leaf area index, total tiller number, dry weights of leave, stem, and panicle, which were determined from three hills with an average number of tillers (Supplementary Data 1). All leaves, stems, and panicles were oven-dried (DHG500, SUPO Co.) at 75°C for several days. We measured N, P, and K contents in

leave, stem and panicle using a continuous flow analyzer (Elementar, Germany), and net photosynthesis of three flag leaves at two photosynthetic photon flux densities of 1500 and 600 μmol m^{-2} s^{-1} using Li6400 (Li-Cor Inc., USA). These measurements were conducted at seedling, maturity, and during three growth phases. Net photosynthesis was measured before and after each rainfall manipulation. In addition, for each treatment, we observed N and P losses via runoff and leaching during the period from the beginning of rainfall manipulation to the time when ponded water level decreased down as that before manipulation.

At maturity, three hills with an average number of panicles were collected from each plot to determine the yield estimated as the product of effective panicles per unit land area (EP), filled grains per panicle (FG), and grain weight (GW) (Supplementary Data 1). The filled grains were oven-dried at 75 °C for at least 72 h, but their weights were adjusted to a fresh weight with a moisture content of 0.15 g H_2O g^{-1}, ref[44]. To determine actual yields, the filled grains from the other rice plant hills for all plots were machine-threshed (OUGEDA Co., China) and sun-dried to reach a moisture content of 0.15 g H_2O g^{-1}. The yields for all plots were highly consistent with actual ones (Supplementary Fig. 20).

We calculated absolute differences in rice yield and in yield components between the controls and treatments, and then converted the absolute differences to relative changes (ΔY, ΔEP, ΔFG, and ΔGW in %) to simplify comparisons among treatments and with

459 the other experimental results. Note that the compensation relationship between ΔEP
460 and ΔFG if rice planting distance below 15 cm (ref[45]) can be avoided in our
461 experimental plots as the distance is 30 cm. ΔY is equal to the sum of ΔEP, ΔFG, and
462 ΔGW, that is ΔY = ΔEP + ΔFG + ΔGW according to the Kaya identity principle[46]. The
463 attribution results help identify the key yield components that were most affected by
464 extreme rainfall. We further identified in which growth phase extreme rainfall regulates
465 the changes in key yield components.
466
467 *1st supplementary experiment*. To isolate the mechanism driving the causal relationship
468 between extreme rainfall and ΔFG, we ran the first supplementary experiment during
469 the reproductive phase in July 2021. In the experiment, extreme rainfall intensity is 103
470 mm per hour (Supplementary Fig. 8 and Data 1). For each treatment, transparent
471 impervious film was placed above half of the plot, such that half of the plants were fully
472 exposed to artificial rainfall and the other part was sheltered but experienced the same
473 increases in ponded water levels and nutrient losses as the exposed part. To avoid an
474 unintentional influence of film on rice growth, the film was also placed above a half
475 control plots and all films were removed when the experiment ended.
476
477 FG and actual yield in exposed and sheltered parts for each plot were observed. Based
478 on the observations, we attributed the effect of extreme rainfall on ΔFG into physical
479 disturbance and soil N loss as below:
480 $$\text{Total: } \Delta Y = Y_{ROC} - Y_{COC}, \Delta FG = FG_{ROC} - FG_{COC}, \quad (2a)$$

481 Soil N loss (o): $\Delta Y_o = Y_{RC} - Y_{CC}$, $\Delta FG_o = FG_{ROC} - FG_{COC}$, (2b)

482 Physical disturbance (p): $\Delta Y_p = \Delta Y - \Delta Y_o$, $\Delta FG_p = \Delta FG - \Delta FG_o$, (2c)

483 where *ROC* and *COC* refer to the exposed parts for treatment and control, respectively.
484 *RC* and *CC* refer to the sheltered parts for treatment and control, respectively. In
485 addition, we measured the number of empty and shrunken grains at maturity as well as
486 their distribution along panicle. Such observations further elucidate how extreme
487 rainfall influences rice pollination during reproductive phase.

488

489 *2nd supplementary experiment*. To confirm the causal effect of extreme rainfall on ΔEP,
490 we ran the second supplementary experiment during vegetative phase in June 2021. The
491 rainfall amount is 240 mm. The experiment consisted of ambient control and two
492 treatments (Supplementary Fig. 8a and Data 1). For treatments, rice plants were fully
493 exposed to artificial rainfall on 6 plots, half of which were re-applied by 28.8 kg N ha^{-1}
494 (37% of tillering fertilizer application) in the form of urea after rainfall manipulation.
495 The re-application rate was determined as the average of observed N losses from the
496 treatment plots using the same rainfall amount during vegetative phase in 2018 and
497 2019.

498

499 For each plot, we observed EP and the actual yield at maturity as well as N uptake per
500 tiller from transplantation to panicle initiation. Based on the observations, we tested the
501 differences in these three indicators between treatments and controls using the
502 Wilcoxon rank sum test. If no significant differences between N re-applied treatment

503 and control but significant differences between normal treatment and control were
504 found, the decrease in EP were attributed to N losses induced by extreme rainfall during
505 the vegetative phase.
506
507 *Path analysis*. Structural equation modelling (SEM) implemented in the R package
508 'lavaan 0.6-7'[47] allows us to test different hypotheses governing the pathways by which
509 extreme rainfall affects rice yield. On the basis of potential causal relationships revealed
510 by our experiments and previous literatures[48-50], a series of SEMs were formulated
511 (Supplementary Fig. 11). The insignificant paths ($P > 0.05$) were eliminated gradually
512 until all links significantly contributed to the final model. To compare model
513 performance, we conducted a chi-squared difference test and calculated model fit
514 statistics (root mean square error of approximation [RMSEA], comparative fit index
515 [CFI], goodness-of-fit index [GFI] and adjusted R squared [R^2_{adj}]). Standardized path
516 coefficients were computed according to ref. [51], which can be interpreted as the change
517 in the dependent variable when the independent variable changes by one standard
518 deviation.
519
520 **Process-based modelling for regional assessments**
521 We improved the process-based crop model ORCHIDEE-crop[23,24,52] to account for the
522 impacts of extreme rainfall according to the mechanisms revealed by our rainfall
523 manipulative experiments. We first tested its performance at the experiment sites driven
524 by climate data observed in 2018 and 2019, and further validated by additional

observations in the supplement experiment year (2021), and then used the improved model to hindcast and project the impacts of extreme rainfall on rice yield across China during 2001-2016 and 2085-2100 under two Representative Concentration Pathways (RCP 4.5 and 8.5).

Model improvement. ORCHIDEE-crop simulates crop phenology, leaf area dynamics, growth of reproductive organs, carbon allocation and managements, as well as carbon, water and energy fluxes of agroecosystems. This model has been applied globally and regionally, and found to robustly reproduce yield variability[53]. ORCHIDE-crop is suitable for this study since it has been optimized for simulating the phenology and yield of single, early and late rice types grown in China[23,52]. It has paddy irrigation and soil hydrology schemes[24], able to represent the typical irrigation and drainage systems for China's rice fields. It runs in a half-hourly time-step and at 0.5-degree grid cell, suitable for extreme rainfall of short duration, which is a challenging issue for the models running at daily time-step.

In ORCHIDEE-crop, the rice growth starts from transplanting (LEV), and the growth cycle includes three stages divided by the onset of grain filling (DRP) and the physiological maturity (MAT)[52]. Starting from DRP, the quantity of dry matters accumulated in grains is calculated by applying a progressive "harvest index" to the biomass of the plant. The daily rate of grain increment is proportional to the daily accumulated thermal unit, which could be reduced by frost and extreme heat[54]. The

impacts of extreme rainfall are formulated as a factor (α) to reduce the rate of grain increment:

$$\alpha = (1 + \Delta EP + \Delta FG), \quad (3a)$$

$$\Delta EP = 0.262 \cdot \Delta N_{ut} - 1.644, \quad (3b)$$

$$\Delta FG = -0.00424 \cdot KE_{re} - 0.00115 \cdot KE_{ri} + 0.139 \cdot \Delta N_{up} - 3.676, \quad (3c)$$

where ΔN_{ut} and ΔN_{up} denote relative change in N uptake per tiller and N uptake per panicle during vegetative phase (%) as a function of soil N losses, respectively. KE_{re} denotes kinetic energy (J m^{-2} h^{-1}) of the maximum hourly precipitation (exceeding the 99th percentile) occurred at 8:00-16:00 in flowering period when spikelets reach anthesis and if hourly air temperature ranges from 23°C to 35°C, ref[55,56]. KE_{ri} denotes kinetic energy of the maximum hourly precipitation (exceeding the 99th percentile) during ripening phase. Note that Equation 3 summing ΔEP and ΔFG is suitable to diagnose and project extreme rainfall induced ΔY across China, because, according to the nationwide survey (Supplementary Data 1), the rice planting distances in China (17 to 25 cm) are enough to avoid the compensation relationship between EP and FG[45]. Further details on model equations can be found in Supplementary Table 4.

Historical simulation. Two sets of historical simulations were performed for three rice types over China: (1) the comprehensive simulation (S0) that accounts both impacts of rainfall-induced physical disturbance and soil N losses on rice yield and (2) the partial simulation (S1) that only accounts the impact of physical disturbance. By comparing S0 and S1, we could isolate the impact of soil N losses. The difference between yield

simulations from the improved and original models can be attributed to the historical extreme rainfall (Supplementary Data 2), thus we derived ΔY as below:

$$\Delta Y = \frac{\text{Yield (improved model) - Yield (original model)}}{\text{Yield (original model)}} \times 100\%. \quad (4)$$

Details on historical input data can be found in Supplementary Table 6. Specifically, we used field observed rice phenology from the CMA to interpolate 0.1-degree transplanting date[52]. We used the satellite-based gridded precipitation datasets (GPM IMERGv6) to quantify extreme rainfall intensities and event amounts, since it is well represented at the site scale (Supplementary Fig. 16).

Future projections. To evaluate the implications of our new findings for future rice yield projections over China, we applied the improved ORCHIDEE-crop to simulate yield changes of three rice types under RCP 4.5 and 8.5 with present-day agricultural management practices (Supplementary Data 2). To analyze the effect of future extreme rainfall on rice yield, we estimated additional rice yield loss as the difference in future projected yields between the improved and original model versions in 2085-2100 relative to the historical yield simulated by the original model in 2001-2016. To remove systematic deviations of the simulated historical climate, we applied the trend-preserving bias-correction[57] to the IPSL projected climate change[30]. The bias correction was then applied to the climate forcing data and extreme rainfall indices during 2085-2100. Further details on input data source for future projections can be found in Supplementary Table 6.

Data availability: The data from the national agrometeorological observation network and the rainfall manipulative experiments are available in Supplementary Data 1. Model input data for historical simulations and future projections are available from public data depositories listed in Supplementary Table 6. Model output data for historical simulations and future projections are available in Supplementary Data 2.

Code availability: Source codes for data analyses are available from https://figshare.com/s/2ab948dda43e73da44b5 (a link for the review but for the public when being accepted). Source codes for process-based model are available from http://forge.ipsl.jussieu.fr/orchidee, under the French Free Software license, compatible with the GNU GPL (http://cecill.info/licences.en.html).

References

1 IPCC. *Managing the Risks of Extreme Events and Disasters to Advance Climate Change Adaptation. A Special Report of Working Groups I and II of the Intergovernmental Panel on Climate Change [Field, C.B., V. Barros, T.F. Stocker, D. Qin, D.J. Dokken, K.L. Ebi, M.D. Mastrandrea, K.J. Mach, G.-K. Plattner, S.K. Allen, M. Tignor, and P.M. Midgley (eds.)]*. (Cambridge University Press, 2012).

2 Ray, D. K., Gerber, J. S., MacDonald, G. K. & West, P. C. Climate variation explains a third of global crop yield variability. *Nat Commun* **6**, 5989, doi:10.1038/ncomms6989 (2015).

3 Lesk, C., Rowhani, P. & Ramankutty, N. Influence of extreme weather disasters on

613 global crop production. *Nature* **529**, 84-87, doi:10.1038/nature16467 (2016).
614 4 Vogel, E. *et al.* The effects of climate extremes on global agricultural yields.
615 *Environ Res Lett* **14**, 054010, doi:10.1088/1748-9326/ab154b (2019).
616 5 Hasegawa, T. *et al.* Extreme climate events increase risk of global food insecurity
617 and adaptation needs. *Nat Food* **2**, 587-595, doi:10.1038/s43016-021-00335-4
618 (2021).
619 6 Lobell, D. B. *et al.* Greater Sensitivity to Drought Accompanies Maize Yield
620 Increase in the US Midwest. *Science* **344**, 516-519, doi:10.1126/science.1251423
621 (2014).
622 7 Lesk, C. *et al.* Stronger temperature-moisture couplings exacerbate the impact of
623 climate warming on global crop yields. *Nat Food* **2**, 683-691, doi:10.1038/s43016-
624 021-00341-6 (2021).
625 8 Wang, X. H. *et al.* Emergent constraint on crop yield response to warmer
626 temperature from field experiments. *Nat Sustain* **3**, 908-916, doi:10.1038/s41893-
627 020-0569-7 (2020).
628 9 Lobell, D. B., Sibley, A. & Ortiz-Monasterio, J. I. Extreme heat effects on wheat
629 senescence in India. *Nat Clim Change* **2**, 186-189,
630 doi:https://doi.org/10.1038/nclimate1356 (2012).
631 10 Zhang, J. Y., Li, X. M., Lin, H. X. & Chong, K. Crop Improvement Through
632 Temperature Resilience. *Annu Rev Plant Biol* **70**, 753-780, doi:10.1146/annurev-
633 arplant-050718-100016 (2019).
634 11 Lesk, C., Coffel, E. & Horton, R. Net benefits to US soy and maize yields from

635 intensifying hourly rainfall. *Nat Clim Change* **10**, 819-822, doi:10.1038/s41558-
636 020-0830-0 (2020).
637 12 Li, Y., Guan, K. Y., Schnitkey, G. D., DeLucia, E. & Peng, B. Excessive rainfall
638 leads to maize yield loss of a comparable magnitude to extreme drought in the
639 United States. *Global Change Biol* **25**, 2325-2337, doi:10.1111/gcb.14628 (2019).
640 13 Webber, H. *et al.* Diverging importance of drought stress for maize and winter
641 wheat in Europe. *Nat Commun* **9**, 1-10, doi:https://doi.org/10.1038/s41467-018-
642 06525-2 (2018).
643 14 Seneviratne, S. I. *et al. Weather and Climate Extreme Events in a Changing*
644 *Climate. In: Climate Change 2021: The Physical Science Basis. Contribution of*
645 *Working Group I to the Sixth Assessment Report of the Intergovernmental Panel on*
646 *Climate Change*. (Cambridge University Press, 2021).
647 15 FAOSTAT, *Crops and livestock products*, Food and Agriculture Organization of the
648 United Nations (FAO) (2019), Date accessed: 20th September 2019,
649 http://www.fao.org/faostat/en/#home.
650 16 Yoshida, S. *Foundations of rice crop science*. 65-69 (International Rice Research
651 Institute, 1981).
652 17 Yuan, S. *et al.* Sustainable intensification for a larger global rice bowl. *Nat*
653 *Commun* **12**, 7163, doi:https://doi.org/10.1038/s41467-021-27424-z (2021).
654 18 Peng, S. S. *et al.* Afforestation in China cools local land surface temperature. *P*
655 *Natl Acad Sci USA* **111**, 2915-2919, doi:10.1073/pnas.1315126111 (2014).
656 19 Win, A., Tanaka, T. S. T. & Matsui, T. Panicle inclination influences pollination

stability of rice (Oryza sativa L.). *Plant Prod Sci* **23**, 60-68, doi:10.1080/1343943x.2019.1698971 (2020).

20 Tian, J. & Huo, Z. G. Index and loss estimation of rain washing damage to early rice pollen in Jiangxi Province. *Journal of Applied Meteorology Science* **29**, 657-666, doi:10.11898/1001-7313.20180602 (2018).

21 Steiner, J. L., Briske, D. D., Brown, D. P. & Rottler, C. M. Vulnerability of Southern Plains agriculture to climate change. *Climatic Change* **146**, 201-218, doi:10.1007/s10584-017-1965-5 (2018).

22 Liu, Y. Q. *et al.* Genomic basis of geographical adaptation to soil nitrogen in rice. *Nature* **590**, 600-605, doi:10.1038/s41586-020-03091-w (2021).

23 Wang, X. H. *Impacts of environmental change on rice ecosystems in China: Development, optimization and application of ORCHIDEE-CROP model (Ph.D. Thesis)*, Peking University, (2016).

24 Yin, Z. *et al.* Improvement of the Irrigation Scheme in the ORCHIDEE Land Surface Model and Impacts of Irrigation on Regional Water Budgets Over China. *J Adv Model Earth Sy* **12**, e2019MS001770, doi:https://doi.org/10.1029/2019MS001770 (2020).

25 Huffman, G. J., Stocker, E. F., Bolvin, D. T., Nelkin, E. J. & Tan, J., *GPM IMERG Final Precipitation L3 Half Hourly 0.1 degree x 0.1 degree V06, Greenbelt, MD*, Goddard Earth Sciences Data and Information Services Center (GES DISC) (2019), Date accessed: 5th August 2021, https://disc.gsfc.nasa.gov/datasets/GPM_3IMERGHH_06/summary.

679 26 Cui, X. Q. *et al.* Global mapping of crop-specific emission factors highlights
680 hotspots of nitrous oxide mitigation. *Nat Food* **2**, 886-893, doi:10.1038/s43016-
681 021-00384-9 (2021).
682 27 Jian, Y. W., Fu, J., Li, B. G. & Zhou, F. Increased extreme hourly precipitation over
683 China's rice paddies from 1961 to 2012. *Sci Rep-Uk* **10**, 10609,
684 doi:https://doi.org/10.1038/s41598-020-67429-0 (2020).
685 28 Rosenzweig, C. *et al.* Assessing agricultural risks of climate change in the 21st
686 century in a global gridded crop model intercomparison. *P Natl Acad Sci USA* **111**,
687 3268-3273, doi:10.1073/pnas.1222463110 (2014).
688 29 Jägermeyr, J. *et al.* Climate impacts on global agriculture emerge earlier in new
689 generation of climate and crop models. *Nat Food* **2**, 873-885, doi:10.1038/s43016-
690 021-00400-y (2021).
691 30 Yang, H., Jiang, Z. H. & Li, L. Biases and improvements in three dynamical
692 downscaling climate simulations over China. *Clim Dynam* **47**, 3235-3251,
693 doi:10.1007/s00382-016-3023-9 (2016).
694 31 Chen, W. L., Jiang, Z. H., Li, L. & Yiou, P. Simulation of regional climate change
695 under the IPCC A2 scenario in southeast China. *Clim Dynam* **36**, 491-507,
696 doi:10.1007/s00382-010-0910-3 (2011).
697 32 Choi, W. J., Lee, M. S., Choi, J. E., Yoon, S. & Kim, H. Y. How do weather
698 extremes affect rice productivity in a changing climate? An answer to episodic lack
699 of sunshine. *Global Change Biol* **19**, 1300-1310,
700 doi:https://doi.org/10.1111/gcb.12110 (2013).

33 Reichstein, M. *et al.* Climate extremes and the carbon cycle. *Nature* **500**, 287-295, doi:https://doi.org/10.1038/nature12350 (2013).

34 Mäkinen, H. *et al.* Sensitivity of European wheat to extreme weather. *Field Crop Res* **222**, 209-217, doi:https://doi.org/10.1016/j.fcr.2017.11.008 (2018).

35 Iizumi, T. *et al.* Prediction of seasonal climate-induced variations in global food production. *Nat Clim Change* **3**, 904-908, doi:https://doi.org/10.1038/nclimate1945 (2013).

36 Meier, J., Zabel, F. & Mauser, W. A global approach to estimate irrigated areas - a comparison between different data and statistics. *Hydrol Earth Syst Sc* **22**, 1119-1133, doi:10.5194/hess-22-1119-2018 (2018).

37 Beillouin, D., Schauberger, B., Bastos, A., Ciais, P. & Makowski, D. Impact of extreme weather conditions on European crop production in 2018. *Philos T R Soc B* **375**, 20190510, doi:http://doi.org/10.1098/rstb.2019.0510 (2020).

38 Nath, H. K. & Mandal, R. Heterogeneous Climatic Impacts on Agricultural Production: Evidence from Rice Yield in Assam, India. *Asian J Agric Dev* **15**, 23-42, doi:10.22004/ag.econ.275687 (2018).

39 Shi, W. J., Wang, M. L. & Liu, Y. T. Crop yield and production responses to climate disasters in China. *Sci Total Environ* **750**, 141147, doi:10.1016/j.scitotenv.2020.141147 (2021).

40 Troy, T. J., Kipgen, C. & Pal, I. The impact of climate extremes and irrigation on US crop yields. *Environ Res Lett* **10**, 054013, doi:https://doi.org/10.1088/1748-9326/10/5/054013 (2015).

41 Abbas, S. & Mayo, Z. A. Impact of temperature and rainfall on rice production in Punjab, Pakistan. *Environ Dev Sustain* **23**, 1706-1728, doi:10.1007/s10668-020-00647-8 (2021).

42 Davis, K. F., Chhatre, A., Rao, N. D., Singh, D. & DeFries, R. Sensitivity of grain yields to historical climate variability in India. *Environ Res Lett* **14**, 064013, doi:10.1088/1748-9326/ab22db (2019).

43 Wu, X. S. *et al.* On the event-based extreme precipitation across China: Time distribution patterns, trends, and return levels. *J Hydrol* **562**, 305-317, doi:10.1016/j.jhydrol.2018.05.028 (2018).

44 Yoon, D. K. *et al.* Transgenic rice overproducing Rubisco exhibits increased yields with improved nitrogen-use efficiency in an experimental paddy field. *Nat Food* **1**, 134-139, doi:10.1038/s43016-020-0033-x (2020).

45 Gravois, K. A. & Helms, R. S. Effect of Uneven Emergence on Rice Yield, Milling Yield, and Yield Components. *Aust J Exp Agr* **34**, 949-952, doi:Doi 10.1071/Ea9940949 (1994).

46 Wang, S. A. *et al.* Reduced sediment transport in the Yellow River due to anthropogenic changes. *Nat Geosci* **9**, 38-41, doi:10.1038/Ngeo2602 (2016).

47 Lefcheck, J. S. PIECEWISESEM: Piecewise structural equation modelling in R for ecology, evolution, and systematics. *Methods Ecol Evol* **7**, 573-579, doi:10.1111/2041-210x.12512 (2016).

48 Ye, T. H. *et al.* Nitrogen, phosphorus, and potassium fertilization affects the flowering time of rice (Oryza sativa L.). *Glob Ecol Conserv* **20**, e00753,

745 doi:10.1016/j.gecco.2019.e00753 (2019).
746 49 Drummond, R. S. M. *et al.* Environmental Control of Branching in Petunia. *Plant*
747 *Physiol* **168**, 735-751, doi:10.1104/pp.15.00486 (2015).
748 50 Ishibashi, M. & Terashima, I. Effects of Continuous Leaf Wetness on
749 Photosynthesis - Adverse Aspects of Rainfall. *Plant Cell Environ* **18**, 431-438,
750 doi:10.1111/j.1365-3040.1995.tb00377.x (1995).
751 51 Bollen, K. A. Total, direct, and indirect effects in structural equation models.
752 *Sociological Methodology* **17**, 37-69, doi:10.2307/271028 (1987).
753 52 Wang, X. H. *et al.* Management outweighs climate change on affecting length of
754 rice growing period for early rice and single rice in China during 1991-2012. *Agr*
755 *Forest Meteorol* **233**, 1-11, doi:10.1016/j.agrformet.2016.10.016 (2017).
756 53 Müller, C. *et al.* Global gridded crop model evaluation: benchmarking, skills,
757 deficiencies and implications. *Geosci Model Dev* **10**, 1403-1422,
758 doi:10.5194/gmd-10-1403-2017 (2017).
759 54 Wu, X. *et al.* ORCHIDEE-CROP (v0), a new process-based agro-land surface
760 model: model description and evaluation over Europe. *Geosci Model Dev* **9**, 857-
761 873, doi:10.5194/gmd-9-857-2016 (2016).
762 55 Kobayasi, K., Matsui, T., Yoshimoto, M. & Hasegawa, T. Effects of Temperature,
763 Solar Radiation, and Vapor-Pressure Deficit on Flower Opening Time in Rice.
764 *Plant Prod Sci* **13**, 21-28, doi:10.1626/pps.13.21 (2010).
765 56 Julia, C. & Dingkuhn, M. Variation in time of day of anthesis in rice in different
766 climatic environments. *Eur J Agron* **43**, 166-174, doi:10.1016/j.eja.2012.06.007

(2012).

57 Hempel, S., Frieler, K., Warszawski, L., Schewe, J. & Piontek, F. A trend-preserving bias correction - the ISI-MIP approach. *Earth Syst Dynam* **4**, 219-236, doi:10.5194/esd-4-219-2013 (2013).

Acknowledgements

This study was supported by the National Natural Science Foundation of China (41977082, F.Z.; 42007079, J.F.; 42171096, X.H.W.; 41530528, S.L.P). We acknowledge Kaiwen Liu, Sheng Wang, Wulahati Adalibieke, Yan Bo, Changxian Wu, Wenjun Jiang, Jianping Wang, Lanying Shu, Xinyi Huang, Lian Chen, Daoheng Zhuang, Chunshan Li, Meishuai Yuan, Hongwei Cai, Chengjie Wang for supporting field experiments and laboratory analyses. We acknowledge the CMA for nationwide observations of rice yield, phenology, hourly precipitation, and extreme climate events, the NASA for GPM IMERGv6 data.

Author contributions

F.Z. designed the study. Y.W.J., J.F. and X.H.W. performed all computational analyses. F.Z., X.H.W., J.F. and Y.W.J. drafted the paper. L.L. provided high-resolution climate projection using the IPSL model. All co-authors reviewed and commented on the manuscript.

Competing interests

The authors declare no competing interests.